Chinese Chemical Letters 32 (2021) 1153–1156

Contents lists available at ScienceDirect

Chinese Chemical Letters

journal homepage: www.elsevier.com/locate/cclet

Communication

A unique 3D microporous MOF constructed by cross-linking 1D coordination polymer chains for effectively selective separation of CO_2/CH_4 and C_2H_2/CH_4

Yu-Pei Xia[a], Chen-Xue Wang[a], Mei-Hui Yu[a,*], Xian-He Bu[a,b,*]

[a] School of Materials Science and Engineering, National Institute for Advanced Materials, Nankai University, Tianjin 300350, China
[b] State Key Laboratory of Elemento-Organic Chemistry, College of Chemistry, Nankai University, Tianjin 300071, China

ARTICLE INFO

Article history:
Received 7 August 2020
Received in revised form 2 September 2020
Accepted 9 September 2020
Available online 10 September 2020

Keywords:
Metal-organic framework
Cross-linking
Selective separation
Dense functional active site

ABSTRACT

Selective separation of CO_2/CH_4 and C_2H_2/CH_4 are promising for their high-purity industrial demand and scientific research on account of the similar molecular radius and physical properties. In this work, a unique 3D microporous MOF material $[Cu(SiF_6)(sdi)_2]$·solvents (**1**, sdi = 1,1′-sulfonyldiimidazole) was successfully constructed by cross-linking 1D coordination polymer chains. The dense functional active sites on the inner walls of the channel of **1a** can provide strong binding affinities to CO_2, C_2H_2, and thus effectively improve the gas separation performance of CO_2/CH_4 and C_2H_2/CH_4.

Selective separation of carbon dioxide (CO_2) and acetylene (C_2H_2) from methane (CH_4) are of significant challenges in natural gas purification and industrial acetylene production [1,2]. However, the conventional porous materials such as zeolites and porous carbons, polymer-based membranes and cryogenic distillation technology cannot meet the requirements for selective separation of the impurities with the similar molecular kinetic diameter (CO_2: 3.3 Å, C_2H_2: 3.3 Å, CH_4: 3.758 Å), boiling point (CO_2: 216.55 K, C_2H_2: 188.40 K, CH_4: 111.66 K) and polarizability (CO_2: 29.11 × 10^{25} cm^{-3}, C_2H_2: 33.3-39.3 × 10^{25} cm^{-3}, CH_4: 25.93 × 10^{25} cm^{-3}) [3]. Moreover, the low efficiency and high energy consumption during the separation process also made them less compatible [4]. Therefore, the development of new materials for CO_2/CH_4 and C_2H_2/CH_4 separation are of great needs.

Metal-organic frameworks (MOFs), as crystalline porous materials, have been widely studied in the areas of gas storage and separation [5–9], luminescent sensing [10–12], heterogeneous catalysis and electrochemistry [13–15]. Benefiting from their unique structures, MOFs are regarded as ideal materials for effectively binding and selective separation of CO_2/CH_4 and C_2H_2/CH_4. Moreover, the rich active heteroatoms sites and open metal sites (OMSs) can enhance the preferential binding of specific guest molecules. For instance, He *et al*. reported a rare Pb_9-cluster MOF based on a flexible cyclotriphosphazene-functionalized hexacarboxylate ligand for gas separation [16]. Owing to the rich active heteroatoms sites and OMSs on the inner pore surfaces of the MOF, the adsorption selectivities of the MOF for the equimolar CO_2/CH_4 and C_2H_2/CH_4 at 298 K and 100 kPa calculated by the predicted ideal adsorbed solution theory (IAST) are 5.8 and 21.0, respectively. However, it should be noted that the rational predesign and construction of MOF materials containing specific microporous and multiple functional active sites (OMS, -NH_2, -F, -OH and *etc*.) are still challenging [17–19]. On one hand, the various coordination modes of both center metal ions and organic ligands make it complicated to predict the final structures of the self-assembly MOFs; On the other hand, the obtained MOF materials may not be applicable to the gas separation on account of the unsuitable aperture of MOF channels and the lack of functional active sites for binding with gas molecules.

In order to tackle the intractable problem, we promoted a cross-linking strategy for the construction of porous MOF materials with multifunctional active sites for effectively selective separation of gas mixtures. A previously reported coordination polymer (CP) $[Cu(sdi)_2(NO_3)_2]$·$2CO(CH_3)_2$ was a representative example for illustrating the strategy [20]. In the titled CP, the one-dimensional (1D) infinite coordinate chains are held together to form three-dimensional (3D) supramolecular structure *via* hydrogen-bonding and Van der Waals interactions. It is worth noting that these 1D chains possess large amounts of terminal coordinated NO_3^- moieties with the hexa-coordinated metal Cu(II) ions. Inspired by this, if the initial metal salt was changed from $Cu(NO_3)_2$·$3H_2O$ to

* Corresponding authors at: School of Materials Science and Engineering, National Institute for Advanced Materials, Nankai University, Tianjin 300350, China.
E-mail addresses: mh@nankai.edu.cn (M.-H. Yu), buxh@nankai.edu.cn (X.-H. Bu).

https://doi.org/10.1016/j.cclet.2020.09.014
1001-8417/

$CuSiF_6{\cdot}nH_2O$, then the SiF_6^{2-} moieties were expected to instead of the terminal NO_3^-, and ultimately these separated 1D chains would be cross-linked by the SiF_6^{2-} moieties to build a novel microporous 3D network (Scheme 1). In addition, the SiF_6^{2-} moieties can also act as functional active sites to facilitate the selective separation of gas molecules, which is proved by previously reported works [21,22].

With this in mind, we successfully constructed a 3D microporous MOF material $[Cu(SiF_6)(sdi)_2]$·solvents (**1**). Compound **1** possessed one-dimensional (1D) narrow channels along the *c* direction, and large amounts of O and F donor sites originated from $-SO_2-$ and SiF_6^{2-} on the inner walls of the channels. These dense functional active sites can provide strong binding affinities to specific guest molecules, and thus effectively improve the gas separation performance. Gas adsorption experiments proved that **1a** (activated **1**) has high adsorption capacity and selectivity for CO_2/CH_4 and C_2H_2/CH_4. In addition, the MOF exhibits high stability not only in common organic solvents but also in deionized water, which is beneficial to its practical and industrial applications.

Single-crystal X-ray diffraction measurement reveals that compound **1** crystallized in the trigonal system with the $R\,\bar{3}\,c$ space group. The asymmetric unit of **1** contains one crystallographically independent sdi ligand, one half of Cu(II) cation and SiF_6^{2-} anion. As shown in Fig. 1a, the Cu(II) centre is hexa-coordinated with four nitrogen atoms originated from four different sdi ligands and two fluorine atoms provided by two SiF_6^{2-} anions. The Cu-N and Cu-F bond distances are in the normal range of 1.988(2)-2.4472(19) Å, which are comparable to the other similar MOFs reported in the previously published papers [23–25]. The selected bond length and angles are listed in Table S2 (Supporting information). Each sdi ligand is coordinated with two Cu(II) ions and connected with another one sdi ligand to generate a $[Cu_2sdi_2]$ unit, and the adjacent units by sharing Cu(II) ions to form an infinite 1D chain (Fig. 1b). Finally, the 1D chains are further cross-linked by SiF_6^{2-} groups to form a 3D honeycomb-like structure with 1D narrow channels along the *c* axis (Figs. 1c and d). The pore limiting diameter of **1** is around 3.4 Å viewed from *c* axis and the potentially free volume (without the solvent molecules) estimated by PLATON program is 25.9%. In order to better understand the complicated structure of **1**, ToposPro software is applied to simplify the specific structure [26]. Based on the simplification, compound **1** can be regarded as a novel 4-connected unimodal *nbo* PLATON program is 25.9 of $\{6^4.8^2\}$ (Fig. 1e).

The purity of **1** was proved by PXRD. As shown in Fig. S2 (Supporting information), the observed PXRD pattern matched well to the simulated one, indicating the bulk sample of **1** possessed good phase purity. TGA curve reveals that **1** has moderate thermal stability and can keep its structure until 230 °C. In addition, **1** can maintain its pristine crystal structure not only in common organic solvents (MeOH, EtOH, CH_3COCH_3, DMF, DMAC, DMSO, CH_3CN, CH_2Cl_2, $CHCl_3$), but also in deionized water for three days, which enhances its potential for practical application (Fig. S3 in Supporting information).

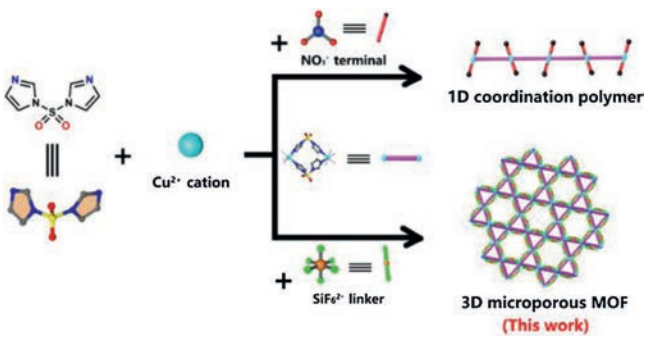

Scheme 1. Schematic for the cross-linking construction of the 3D microporous MOF.

Based on the good stability of **1**, N_2 adsorption experiment was performed at 77 K to evaluate the porosity of **1a**. As illustrated in Fig. S4 (Supporting information), negligible N_2 was adsorbed. The sample was collected after the N_2 sorption measurement for further inspection. PXRD testing confirmed that the framework of **1a** did not collapse (Fig. S2), so the low N_2 uptake of **1a** can be attributed to the repulsion of the framework to N_2 and the small aperture size hindered the N_2 molecules into the channels of **1a** under this circumstance. Subsequently, we changed the probe molecule to CO_2 because of its small kinetic diameter (3.30 Å) compared to N_2 (3.64 ~ 3.80 Å). As expected, a high uptake amount of CO_2 with type I isotherm was observed at 195 K (saturated capacity: 101.2 cm^3/g, Fig. S4). The experimental pore volume of **1a** is 0.1512 cm^3/g. The Brunauer-Emmett-Teller (BET) surface area and Langmuir surface area of **1a** were calculated to be 358 m^2/g and 442 m^2/g based on the CO_2 adsorption experiment, respectively [27,28].

The microporous structure with relatively high BET surface area, multiple functional active sites and high stability prompted us to investigate the gas sorption and separation properties of **1a**. CO_2, C_2H_2 and CH_4 were selected as the targeted molecules on account of their high-purity industrial demand and scientific research. The single-component adsorption experiments of **1a** toward CO_2, C_2H_2 and CH_4 were measured at 273 K and 298 K, respectively. As illustrated in Fig. 2a, **1a** has relatively high CO_2 and C_2H_2 adsorption capacity (29.2 cm^3/g for CO_2 and 34.2 cm^3/g for C_2H_2) at 298 K and 1 atm. When the temperature is reduced to 273 K, the trend is maintained and the corresponding gas uptakes increased to 45.1 and 48.7 cm^3/g, respectively (Fig. 2b). Compared to CO_2 and C_2H_2, only limited amounts of CH_4 are adsorbed (6.8 cm^3/g at 298 K and 11.7 cm^3/g at 273 K). The distinctly different gas adsorption behaviors indicated that **1a** can act as a promising material for the selective separation of CO_2/CH_4 and C_2H_2/CH_4.

The adsorption selectivities of **1a** towards binary gas mixtures CO_2/CH_4 (50/50, v/v) and C_2H_2/CH_4 (50/50, v/v) were evaluated by the IAST. The Langmuir-Freundlich equation fits extremely well with the single-component isotherms of CO_2, C_2H_2 and CH_4 at 273 and 298 K (Figs. S5-S7 in Supporting information). As shown in Fig. 3, the IAST adsorption selectivities are 10.4 for CO_2/CH_4 and 11.2 for C_2H_2/CH_4 at 298 K. As the temperature lowered to 273 K, the selectivities increased to 12.5 and 17.1, respectively. The IAST selectivities of **1a** towards CO_2/CH_4 (50/50, v/v) and C_2H_2/CH_4 (50/50, v/v) under 298 K are superior to some previously reported MOFs (Table S3 in Supporting information). These results further proved that **1a** is capable for selective separation of CO_2/CH_4 and C_2H_2/CH_4 mixtures.

To elucidate the reason that of compound **1a** exhibits comparatively high adsorption amount and selectivity for CO_2 and C_2H_2, the Q_{st} for **1a** toward the different gas molecules were calculated by the Clausius-Clapeyron equation using isotherm fits to the Virial equation based on the single component gas adsorption isotherms measured at 273 K and 298 K (Figs. S8-S10 in Supporting information). The Q_{st} values at near zero coverage are found to be 31.9, 26.8 and 16.3 kJ/mol for CO_2, C_2H_2 and CH_4, respectively (Fig. S11 in Supporting information). Obviously, the Q_{st} values of CO_2 and C_2H_2 are much higher than that of CH_4, which confirmed the strong affinities between CO_2, C_2H_2 molecules and the framework of **1a**, and thus resulting the highly selective separation of CO_2/CH_4 and C_2H_2/CH_4. The Q_{st} curves for CO_2 and C_2H_2 showed two distinctly different trends, with the increase of gas adsorption, the Q_{st} value for CO_2 decreased, while that for C_2H_2

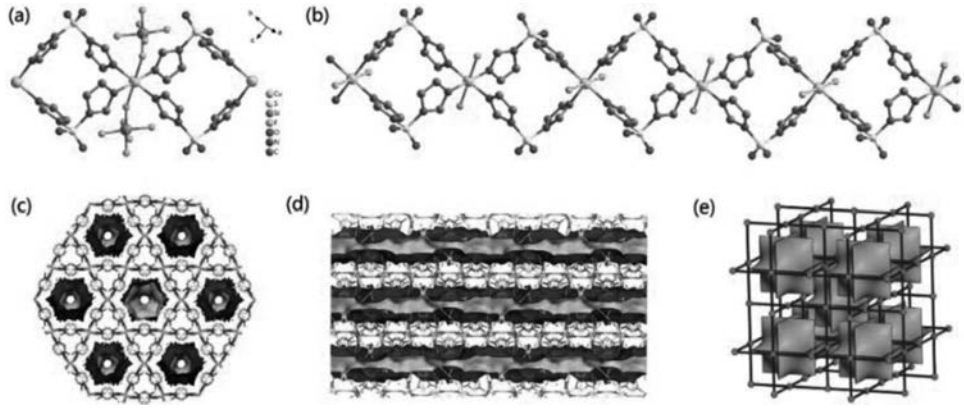

Fig. 1. (a) The coordination environment of the centre Cu(II) ion. (b) The infinite 1D Cu(II)-sdi chain (SiF_6^{2-} groups are omitted for clarity). (c, d) The 3D structure of **1** along *c* and *b* axes (the isosurfaces represent the voids inside the pores). (e) The tiling image of the simplified framework of **1**. Color codes: Cu (sky blue), S (yellow), Si (orange), F (green), O (red), N (mazarine), C (gray). Hydrogen atoms are omitted for clarity.

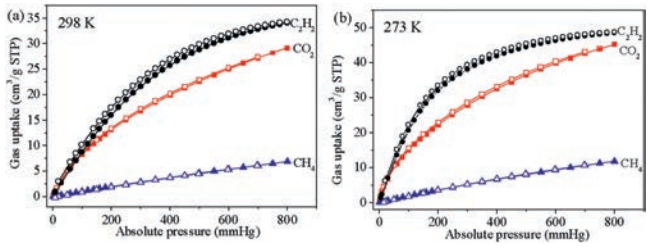

Fig. 2. Single-component adsorption isotherms of C_2H_2 (black), CO_2 (red), CH_4 (blue) of **1a** at (a) 298 K and (b) 273 K.

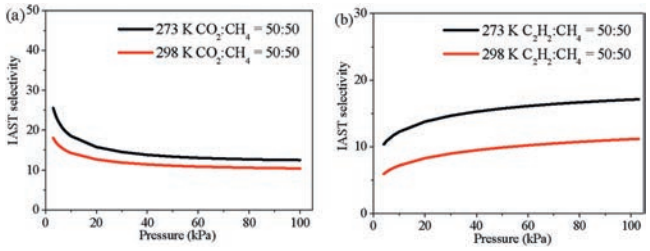

Fig. 3. The IAST adsorption selectivities of CO_2/CH_4 and C_2H_2/CH_4 of **1a** at 273 K (black) and 298 K (red).

increased. These phenomena could be ascribed to the continuously variational intermolecular interactions along with the gas adsorption process [29]. Moreover, the Q_{st} values of both CO_2 and C_2H_2 are comparable to or even surpassing to some well-known MOFs decorated with functional group sites (-NH_2, -F, -OH, *etc.*) and/or OMSs (Table S4 in Supporting information).

Therefore, on the basis of the above analysis, the following aspects can be used as explanation of the preferable adsorption phenomena of **1a**: (a) The small apertures and the repulsion of framework hindered the CH_4 molecules into the pore channels of **1a** [30]; (b) The O and F donor sites originated from the functional active sites (-SO_2- and SiF_6^{2-}) on the inner walls of the channels can provided strong binding affinities *via* hydrogen-bonding and/or Van der Waals interactions with the CO_2 and C_2H_2 molecules [31,32]; (c) CO_2 and C_2H_2 are more easily to be condensed than CH_4 for their relatively higher critical temperature (CO_2: 304.12 K, C_2H_2: 308.3 K, CH_4: 190.56 K) [33]; (d) The higher polarizability of CO_2 and C_2H_2 than CH_4 resulted in stronger interactions between the framework of **1a** and CO_2 or C_2H_2. All these factors contribute to the preferable adsorption of **1a** toward CO_2 and C_2H_2 to CH_4 [34,35].

In summary, a novel 3D MOF material **1** with 1D microporous was rationally designed and constructed by cross-linking 1D coordination polymer chains. The dense functional active sites on the inner walls of the channels can offer strong binding affinities to specific guest molecules, and thus favorable for the gas separation performance. Furthermore, gas adsorption experiments confirm that **1a** have relatively high CO_2 and C_2H_2 adsorption capacities over CH_4 at 1 bar. The predicted IAST adsorption selectivities for CO_2/CH_4 and C_2H_2/CH_4 are 10.4, 11.2 at 298 K and 12.5, 17.1 at 273 K. This work not only reported a porous MOF for effectively selective separation of CO_2/CH_4 and C_2H_2/CH_4, but also opened a new perspective for the rational predesign and functionalization of MOFs materials.

Declaration of competing interest

The authors report no declarations of interest

Acknowledgments

This work was supported by the National Natural Science Foundation of China (NSFC, Nos. 91856124 and 21531005), Nature Science Fund of Tianjin, China (No. 19JCZDJC37200).

Appendix A. Supplementary data

Supplementary material related to this article can be found, in the online version, at doi:https://doi.org/10.1016/j.cclet.2020.09.014.

References

[1] R.B. Lin, S. Xiang, H. Xing, et al., Coord. Chem. Rev. 378 (2019) 87–103.
[2] B. Li, H.M. Wen, Y. Yu, et al., Mater. Today Nano 2 (2018) 21–49.
[3] J.R. Li, R.J. Kuppler, H.C. Zhou, Chem. Soc. Rev. 38 (2009) 1477–1504.
[4] D.S. Sholl, R.P. Lively, Nature 532 (2016) 435–437.
[5] W. Fan, X. Liu, X. Wang, et al., Inorg. Chem. Front. 5 (2018) 2445–2449.
[6] X. Zhao, Y. Wang, D.S. Li, et al., Adv. Mater. 30 (2018) 1705189.
[7] J.W. Zhang, M.C. Hu, S.N. Li, et al., Chem. Commun. 54 (2018) 2012–2015.
[8] G. Si, X. Kong, T. He, et al., Chin. Chem. Lett. 32 (2021) 918-922.
[9] M.H. Yu, B. Space, D. Franz, et al., J. Am. Chem. Soc. 141 (2019) 17703–17712.
[10] J.J. Ma, W.S. Liu, Dalton Trans. 48 (2019) 12287–12295.
[11] W.P. Lustig, S. Mukherjee, N.D. Rudd, et al., Chem. Soc. Rev. 46 (2017) 3242–3285.
[12] Z.Q. Yao, J. Xu, B. Zou, et al., Angew. Chem. Int. Ed. 58 (2019) 5614–5618.
[13] J.-Y. Zhao, R. Wang, S. Wang, et al., J. Mater. Chem. A 7 (2019) 7389–7395.
[14] T. Zhang, W. Lin, Chem. Soc. Rev. 43 (2014) 5982–5993.
[15] J. Liu, L. Chen, H. Cui, et al., Chem. Soc. Rev. 43 (2014) 6011–6061.
[16] D. Bai, F. Chen, D. Jiang, Y. He, Inorg. Chem. Front. 4 (2017) 1501–1508.
[17] J.R. Li, J. Yu, W. Lu, et al., Nat. Commun. 4 (2013) 1538.

[18] B. Liu, S. Yao, C. Shi, et al., Chem. Commun. 52 (2016) 3223–3226.
[19] X. Wang, Y. Zhang, Z. Chang, et al., Chin. J. Chem. 37 (2019) 871–877.
[20] K. Liu, B. Ma, X. Guo, et al., CrystEngComm 17 (2015) 5054–5065.
[21] S.D. Burd, S. Ma, J.A. Perman, et al., J. Am. Chem. Soc. 134 (2012) 3663–3666.
[22] P. Nugent, Y. Belmabkhout, S.D. Burd, et al., Nature 495 (2013) 80–84.
[23] C.H. Springsteen, R.D. Sweeder, R.L. LaDuca, Cryst. Growth Des. 6 (2006) 2308–2314.
[24] V. Guillerm, L. Garzon-Tovar, A. Yazdi, et al., Chem. -Eur. J. 23 (2017) 6829–6835.
[25] D. O'Nolan, A. Kumar, M.J. Zaworotko, J. Am. Chem. Soc. 139 (2017) 8508–8513.
[26] V.A. Blatov, A.P. Shevchenko, D.M. Proserpio, Cryst. Growth Des. 14 (2014) 3576–3586.
[27] S. Brunauer, P.H. Emmett, E. Teller, J. Am. Chem. Soc. 60 (1938) 309–319.
[28] I. Langmuir, J. Am. Chem. Soc. 40 (1918) 1361–1403.
[29] O.T. Qazvini, R. Babarao, Z.L. Shi, et al., J. Am. Chem. Soc. 141 (2019) 5014–5020.
[30] M. Du, C.P. Li, M. Chen, et al., J. Am. Chem. Soc. 136 (2014) 10906–10909.
[31] A. Cadiau, Y. Belmabkhout, K. Adil, et al., Science 356 (2017) 731–735.
[32] H. Li, L. Li, R.B. Lin, et al., ACS Sustain. Chem. Eng. 7 (2019) 4897–4902.
[33] B.E. Poling, J.M. Prausnitz, J.P. O'Connell, The Properties of Gases and Liquids, 5th ed., McGraw-Hill, 2000.
[34] F. Chen, Y. Wang, D. Bai, et al., J. Mater. Chem. A 6 (2018) 3471–3478.
[35] Y. Wang, M. He, X. Gao, et al., Dalton Trans. 47 (2018) 12702–12710.